COMP0212- Modelling and Simulation
Project Report
The Behaviour of Light Around a Black Hole

Group 4
Aayan Islam – 24102520
Xavier Parker – 24077390
Helitha Cooray – 24161798

December 2025

Contents

1 Introduction

1.1 Purpose

The purpose of our project is to examine how light travels around a Black Hole in a 2D world. More specifically to examine what happens to the path light takes when it closes in on the black hole and what makes light more likely to fall in or escape the black hole.

1.2 Importance

The importance of this project stems from a lack of complete understanding of what happens around a black hole. Because it is impossible to actually go to a black hole and run experiments, we are limited to simulation based experiments to gain a deeper understanding of the physics at play.

1.3 Existing Models

Model visualizations of black holes can fall into two complementary categories:

- **Physically based rendering** methods that numerically propagate light rays through spacetime to generate synthetic images.
- **Observational reconstructions** that recover images from telescope measurements using signal processing and statistical inference.

Both methods have shaped general and scientific expectations of what black holes, and the spacetime around them, look like, and they motivate the modelling choices used in this project.

Physically based ray-tracing and cinematic models (Interstellar). A well-known example of a physics-based visualization is the black hole **Gargantua** featured in the film *Interstellar* [1]. Gargantua's appearance was generated using a dedicated renderer developed by the visual effects team at Double Negative, known as the **Double Negative Gravitational Renderer (DNGR)** [2]. This renderer traces light propagation through curved spacetime surrounding a **rotating (Kerr) black hole**, rather than relying on simplified gravitational lensing approximations. By solving the underlying light-transport problem using large bundles of null rays, DNGR was able to generate smooth, high-resolution images suitable for cinematic projection and rapidly changing camera viewpoints. This work is significant as it demonstrates that relativistic ray-tracing can be implemented within a film production pipeline while remaining grounded in the physical principles governing spacetime geometry and photon propagation [3].

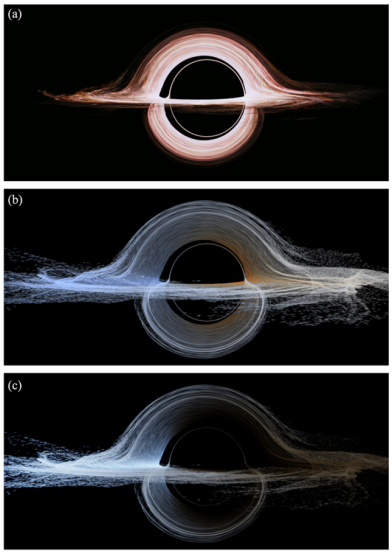

Figure 1: Ray-traced visualization of the black hole Gargantua from *Interstellar*.

Observational imaging models (Event Horizon Telescope). In contrast to forward-rendering approaches, the **Event Horizon Telescope (EHT)** produces images using **inverse modelling** techniques. The EHT combines measurements from a global array of radio

telescopes to form an Earth-sized virtual aperture via very-long-baseline interferometry (VLBI). The first EHT image, released in 2019 revealed a bright ring surrounding a central intensity depression for the supermassive black hole at the centre of galaxy M87 (M87*) [4]. A second landmark result followed in 2022 with the first image of Sagittarius A* (Sgr A*), the supermassive black hole at the centre of the Milky Way [5].

In this case, additional challenges arise due to the rapidly varying emission from the surrounding plasma, requiring reconstruction methods that remain robust under time-dependent behaviour. These observational results provide real-world qualitative benchmarks such as ring structure, brightness asymmetry, and shadow scale—that forward simulations seek to reproduce under physically plausible assumptions.

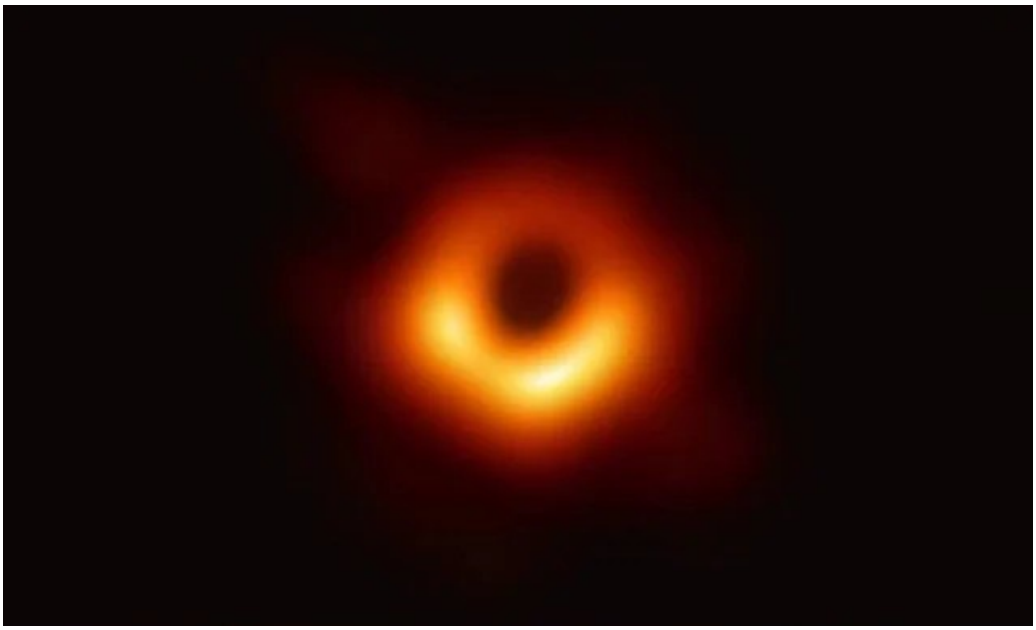

Figure 2: Captured image of the black hole M87.

1.4 Relevance to Course

Although this project does not have any robotics or Artificial Intelligence elements, this project is still relevant to the Modelling & Simulation module. We use ODEs to model the path the light takes, we have Gaussian noise to mimic disturbances around the black hole and we perform Monte Carlo experiments to gather insights. In addition, we have good visualisations, aiding in understanding the physics going on.

2 Theoretical Background

2.1 System description

2.1.1 Light in Space

Unlike in Newtonian physics, where photons would be completely unaffected by mass and therefore gravity, **General Relativity** states that light follows the curvatures of the spacetime "fabric". Near massive bodies like stars or black holes, the spacetime curvature becomes extreme (condensing into a singular, infinitely dense point in the case of a black hole), bending the

paths of photons significantly. The goal of our simulation is to model how a light ray (photon) moves in curved spacetime, described by the **Schwarzschild metric**.

2.1.2 Geodesic Motion

Since the path of a free photon is not determined by forces, their paths, called **geodesics**, represent the "straightest possible" trajectories for light or any free particle in curved spacetime geometry. Mathematically, these paths satisfy the following geodesic equation:

$$\frac{d^2r}{d\lambda^2} = -\Gamma^r_{\alpha\beta}\frac{dx^\alpha}{d\lambda}\frac{dx^\beta}{d\lambda}$$

Here, x^μ represents the four coordinates (t, r, θ, ϕ) of spacetime, λ is an affine parameter (for light, it can be thought of as a parameter along the ray's path), and $\Gamma^\mu_{\alpha\beta}$ are the **Christoffel symbols** that describe the curvature of spacetime around a body. The second term acts like a "gravitational correction" to straight-line motion as it quantifies how spacetime curvature deflects the trajectory. In flat spacetime (no gravity), all $\Gamma^\mu_{\alpha\beta} = 0$, and it reduces to the straight line motion of special relativity.

For light, the spacetime interval ds^2 is **null**, because photons have no rest mass, meaning

$$ds^2 = 0$$

Such trajectories are called **null geodesics**. The null geodesic condition is what distinguishes photons from other particles which have mass. Massive particles follow **time-like geodesics** for which $ds^2 < 0$. The distinction between these types of trajectories is essential in understanding how gravity affects light compared to massive bodies.

2.1.3 Black Holes

Black holes are arguably the most profound prediction of Einstein's theory of General Relativity, describing regions of **spacetime** where gravity is so intense that nothing, not even light, can escape. These bodies are the result of massive stars reaching the end of their lifespan, collapsing under their own gravity, compressing their entire mass into an infinitely small volume called a **singularity**.

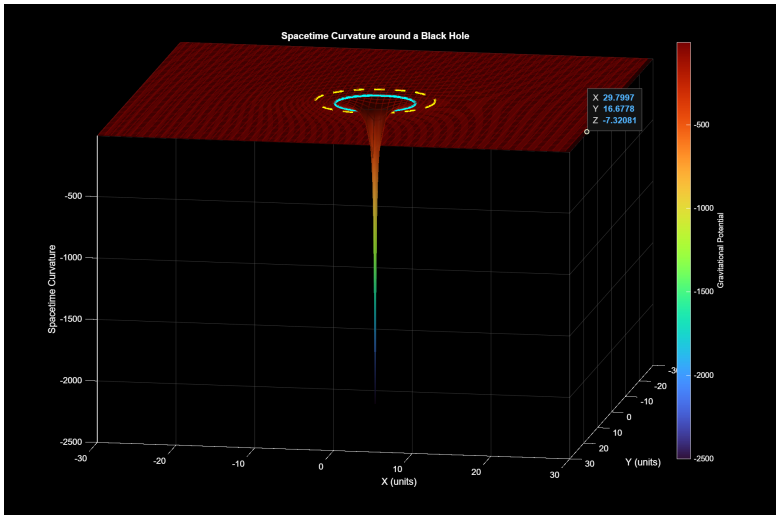

Figure 3: Heatmap of spacetime around a black hole

Figure 3 is our visualisation of the spacetime curvature surrounding a Schwarzchild black hole. Rather than representing a physical embedding of spacetime, the surface is generated using a smooth scalar field of the form

$$Z(r) \propto -\frac{1}{r^n},$$

where $r = \sqrt{x^2 + y^2}$ is the radial distance from the black hole centre (similar to our actual model) and n is a tunable smoothing exponent. This functional form is chosen purely for visual clarity, producing a steep central **"funnel"** that qualitatively conveys the increasing curvature near the singularity. The event horizon (cyan ring) and photon sphere (yellow dashed ring) are overlaid as reference markers, but the surface itself does not encode geodesic motion or relativistic dynamics. All physically meaningful photon trajectories in this report are instead computed from the Schwarzschild metric and null geodesic equations which we will discuss in the following sections of the report.

The defining feature of a black hole is the **event horizon**, a one-way boundary defined by the **Schwarzschild radius**.

$$r_{\mathrm{s}} = \frac{2GM}{c^2}$$

- **Gravitational Constant** (G): determines the **strength of gravity**. It scales the relationship between mass and the resulting curvature of spacetime.
- **Mass** (M): total mass of the black hole. R_s is **directly proportional** to this mass.
- **Speed of Light** (c): The universe's fundamental **speed limit**.

Once matter or light crosses this horizon, it is irrevocably pulled towards the singularity. Within our report's context, modelling the event horizon is crucial, as it is the boundary condition where the spacetime geometry changes, dictating the ultimate path of ingoing light rays. The light rays that travel along null geodesics that are far from black holes will always follow the path of a straight line. However, close to the black hole, these geodesics are dramatically bent, altering the path. This leads to phenomena such as the **photon sphere**, an unstable circular orbit for light around the event horizon. Additionally, light is emitted from a ring-like formation, called the **accretion disc**, which consists of normal matter- mostly gas and dust that spirals into the black hole. This results in the formation of the distinctive and well-recognized **black hole shadow**. Apart from their immense mass, the other properties black holes possess are charge and spin, similar to fundamental particles. For our report, we assume a non-rotating black hole, and therefore, we will be using the **Schwarzchild metric** to understand the visual appearance and behaviour of our simulation.

The Schwarzchild metric describes how intervals in spacetime are measured within the gravitational field of a non-rotating, spherically symmetric mass, as we assume for the simulation. It forms the relationship between **time**, **radial distance**, and **angular position** for any particle moving in this region of curved space time.

$$f(r) = 1 - \frac{r_s}{r}$$

2.2 Methodology

2.2.1 Initial Condition Mapping

Given that the initial position and propagation direction of the light ray are specified in the Cartesian x–y plane, these quantities are converted into polar coordinates to match the Schwarzschild geodesic formulation:

- $r = \sqrt{(x_{\text{pos}})^2 + (y_{\text{pos}})^2}$, which defines the initial radial distance from the black hole.
- $\phi = \arctan(y_{\text{pos}}, x_{\text{pos}})$, giving the initial angular position.
- $\dot{r} = x_{\text{dir}} \cos(\phi) + y_{\text{dir}} \sin(\phi)$, obtained by projecting the Cartesian direction vector onto the radial basis.
- $\dot{\phi} = \dfrac{-x_{\text{dir}} \sin(\phi) + y_{\text{dir}} \cos(\phi)}{r}$, representing the angular velocity component.
- $L = r^2\dot{\phi}$, the conserved angular momentum per unit energy of the photon.
- $f = 1 - \dfrac{r_s}{r}$, the Schwarzschild metric factor encoding spacetime curvature.
- $\dfrac{dt}{d\lambda} = \sqrt{\dfrac{\dot{r}^2}{f^2} + \dfrac{r^2\dot{\phi}^2}{f}}$, obtained from the null geodesic condition $ds^2 = 0$.
- $E = f \cdot \dfrac{dt}{d\lambda}$, the conserved energy-like quantity associated with time-translation symmetry.

2.2.2 State-Space Representation

To make numerical integration possible, we formulate the governing geodesic equations as a first-order state space system. The system state vector is defined as:

$$\mathbf{X} = \begin{bmatrix} r \\ \phi \\ \dot{r} \\ \dot{\phi} \end{bmatrix}$$

where r and ϕ represent the photon's instantaneous radial and angular position, and $\dot{r}$, $\dot{\phi}$ are derivatives with respect to the affine parameter λ. With our state space model, we can solve our geodesic equations using a standard numerical ODE solver. The resulting system is fully deterministic in the absence of stochastic perturbations and evolves following solely the curvature of spacetime defined by the Schwarzschild metric. This state-space approach gives us a modular framework in which additional physical effects, such as noise or external factors, can be systematically introduced without altering the core dynamics of the system.

Setup

We derive the radial component of the null geodesic equation ($\frac{d^2r}{d\lambda^2}$) using the **Christoffel symbols** for the Schwarzschild metric. We assume motion is confined to the equatorial plane ($\theta = \pi/2$, $d\theta/d\lambda = 0$) and set the speed of light $c = 1$. The metric components use $f(r) = 1 - r_s/r$, where r_s is the Schwarzschild radius.

- **Schwarzschild equation:**

$$ds^2 = -\left(1 - \frac{r_s}{r}\right) c^2 \left(\frac{dt}{d\lambda}\right)^2 \quad + \quad \left(1 - \frac{r_s}{r}\right)^{-1} \left(\frac{dr}{d\lambda}\right)^2 \quad + \quad r^2 \left(\frac{d\phi}{d\lambda}\right)^2$$

- **Schwarzschild equation after simplification:**

$$ds^2 = (-f) \left(\frac{dt}{d\lambda}\right)^2 \quad + \quad (f)^{-1} \left(\frac{dr}{d\lambda}\right)^2 \quad + \quad r^2 \left(\frac{d\phi}{d\lambda}\right)^2$$

- **Schwarzschild Metric Components:**

$$g_{tt} = -f \quad ; \quad g_{rr} = f^{-1} \quad ; \quad g_{\phi\phi} = r^2$$

- **Inverse Metric Component:**

$$g^{tt} = -\frac{1}{f} \quad ; \quad g^{rr} = f \quad ; \quad g^{\phi\phi} = \frac{1}{r^2}$$

2.2.3 The Geodesic Equation

The geodesic equation for the r-component ($\mu = r$) is:

$$\frac{d^2 r}{d\lambda^2} = -\Gamma^r_{\alpha\beta} \frac{dx^\alpha}{d\lambda} \frac{dx^\beta}{d\lambda}$$

Since the metric is diagonal, the equation simplifies to:

$$\frac{d^2 r}{d\lambda^2} = -\left[\Gamma^r_{tt} \left(\frac{dt}{d\lambda}\right)^2 + \Gamma^r_{rr} \left(\frac{dr}{d\lambda}\right)^2 + \Gamma^r_{\phi\phi} \left(\frac{d\phi}{d\lambda}\right)^2\right] \tag{1}$$

2.2.4 Calculation of Christoffel Symbols ($\Gamma^r_{\alpha\beta}$)

The general formula for Christoffel symbols in a diagonal metric is $\Gamma^\mu_{\alpha\beta} = \frac{1}{2} g^{\mu\mu} \left(\frac{\partial g_{\mu\alpha}}{\partial x^\beta} + \frac{\partial g_{\mu\beta}}{\partial x^\alpha} - \frac{\partial g_{\alpha\beta}}{\partial x^\mu}\right)$.

1. **The Gravity Term (Γ^r_{tt})** This term is derived from $\Gamma^r_{tt} = -\frac{1}{2} g^{rr} \frac{\partial g_{tt}}{\partial r}$.

   - **Derivative of g_{tt}:**

$$g_{tt} = -1 + \frac{r_s}{r} \implies \frac{\partial g_{tt}}{\partial r} = \frac{\partial}{\partial r}\left[r_s r^{-1}\right] = -\frac{r_s}{r^2}$$

   - **Christoffel Symbol:**

$$\Gamma^r_{tt} = -\frac{1}{2}(f)\left(-\frac{r_s}{r^2}\right) = +\frac{\mathbf{r_s f}}{\mathbf{2r^2}}$$

2. **The Radial Curvature Term (Γ^r_{rr})** This term is derived from $\Gamma^r_{rr} = \frac{1}{2} g^{rr} \frac{\partial g_{rr}}{\partial r}$.

   - **Derivative of g_{rr}:**

$$g_{rr} = f^{-1} \implies \frac{\partial g_{rr}}{\partial r} = -1 f^{-2} \left(\frac{r_s}{r^2}\right) = -\frac{r_s}{r^2 f^2}$$

   - **Christoffel Symbol:**

$$\Gamma^r_{rr} = \frac{1}{2}(f)\left(-\frac{r_s}{r^2 f^2}\right) = -\frac{\mathbf{r_s}}{\mathbf{2r^2 f}}$$

3. The Centrifugal Term ($\Gamma^r_{\phi\phi}$) This term is derived from $\Gamma^r_{\phi\phi} = -\frac{1}{2}g^{rr}\frac{\partial g_{\phi\phi}}{\partial r}$.

- **Derivative of $g_{\phi\phi}$:**

$$g_{\phi\phi} = r^2 \implies \frac{\partial g_{\phi\phi}}{\partial r} = 2r$$

- **Christoffel Symbol:**

$$\Gamma^r_{\phi\phi} = -\frac{1}{2}(f)(2r) = -rf = -(\mathbf{r} - \mathbf{r_s})$$

2.2.5 Calculation of Angular Geodesic Acceleration ($\frac{d^2\phi}{d\lambda^2}$)

The angular component of the geodesic equation ($\mu = \phi$) is:

$$\frac{d^2\phi}{d\lambda^2} = -\Gamma^\phi_{\alpha\beta}\frac{dx^\alpha}{d\lambda}\frac{dx^\beta}{d\lambda} \tag{2}$$

Since the Schwarzschild metric is static and spherically symmetric, the only non-zero Christoffel symbols for $\mu = \phi$ are when one index is r and the other is ϕ. Since $\Gamma^\phi_{r\phi} = \Gamma^\phi_{\phi r}$, the equation simplifies to:

$$\frac{d^2\phi}{d\lambda^2} = -2\Gamma^\phi_{r\phi}\left(\frac{dr}{d\lambda}\right)\left(\frac{d\phi}{d\lambda}\right)$$

4. The Angular Term ($\Gamma^\phi_{r\phi}$) This term is derived from $\Gamma^\phi_{r\phi} = \frac{1}{2}g^{\phi\phi}\left(\frac{\partial g_{\phi r}}{\partial \phi} + \frac{\partial g_{\phi\phi}}{\partial r} - \frac{\partial g_{r\phi}}{\partial \phi}\right)$, which simplifies since $g_{r\phi} = 0$:

$$\Gamma^\phi_{r\phi} = \frac{1}{2}g^{\phi\phi}\frac{\partial g_{\phi\phi}}{\partial r}$$

- **Inverse Metric and Derivative:**

$$g^{\phi\phi} = \frac{1}{r^2} \quad \text{and} \quad \frac{\partial g_{\phi\phi}}{\partial r} = 2r$$

- **Christoffel Symbol:**

$$\Gamma^\phi_{r\phi} = \frac{1}{2}\left(\frac{1}{r^2}\right)(2r) = \mathbf{\frac{1}{r}}$$

Angular Geodesic Equation

Substituting $\Gamma^\phi_{r\phi}$ back into the simplified geodesic equation:

$$\frac{d^2\phi}{d\lambda^2} = -2\left(\frac{1}{r}\right)\left(\frac{dr}{d\lambda}\right)\left(\frac{d\phi}{d\lambda}\right)$$

$$\mathbf{\frac{d^2\phi}{d\lambda^2} = -\frac{2}{r}\frac{dr}{d\lambda}\frac{d\phi}{d\lambda}}$$

2.2.6 Final Geodesic Equations

The coupled differential equations for the radial and angular motion are:

- **Radial Acceleration ($\frac{d^2r}{d\lambda^2}$):**

$$\frac{d^2r}{d\lambda^2} = -\frac{\mathbf{r_s}}{\mathbf{2r^2\,(f)}}\left(\frac{\mathbf{dt}}{\mathbf{d\lambda}}\right)^{\mathbf{2}} \quad + \quad \frac{\mathbf{r_s}}{\mathbf{2r^2\,(f)}}\left(\frac{\mathbf{dr}}{\mathbf{d\lambda}}\right)^{\mathbf{2}} \quad + \quad \mathbf{(r-r_s)}\left(\frac{\mathbf{d\phi}}{\mathbf{d\lambda}}\right)^{\mathbf{2}}$$

  where $\mathbf{f} = 1 - \frac{r_s}{r}$

- **Angular Acceleration ($\frac{d^2\phi}{d\lambda^2}$):**

$$\frac{d^2\phi}{d\lambda^2} = -\frac{\mathbf{2}}{\mathbf{r}}\frac{\mathbf{dr}}{\mathbf{d\lambda}}\frac{\mathbf{d\phi}}{\mathbf{d\lambda}}$$

2.2.7 Stochasticity and randomness

To account for **stochasticity and randomness**, we added **random Gaussian noise** in the f variable, as well as the second derivative of r and ϕ. Without noise, we model the Schwarzschild solution as an idealized, perfectly static spacetime. However, this does not account for real-world measurements and environments that can cause uncertainties. Rather than having the Gaussian noise represent "literal" randomness in spacetime, these perturbations can serve as a proxy for unresolved physical factors such as magnetic fields and gravitational influence from other nearby celestial bodies, or small-scale spacetime fluctuations ignored in the ideal Schwarzchild solution. Introducing Gaussian noise accounts for these unknown factors, ensuring the simulated light ray is not just a single fixed calculation, while preserving the underlying system, allowing us to explore the model behaviour without violating the constraints of the null geodesic equations

2.2.8 Assumptions

The main assumption of this project was that we assumed that $G(6.67\times10^{-11}) = c(3\times10^{8}) = 1$. This conversion allows us to make use of geometrize units where everything is expressed within the same unit system.

While this may appear to be an unreasonable equality given that the numbers are so vastly different, the reason lies within the equations used for modelling the rays of light. By using this assumption, many very large and small numbers are removed from the equation, reducing equation complexity and making it easier to work out the equations for the state model. This also means that in MATLAB, there are less extreme numbers being used with prevents the chance of overflow or underflow errors which ensures there is no numerical instability.

Additionally, by using these geometrize units, we are able to focus on the physical behaviour of the rays of light rather than the conversion of units. During initial development of the simulation, this assumption was not used which lead to plots having values with a magnitude of around 10^{22} on both the axes which made it very difficult to view what the actual ray of light was doing. By reducing equation complexity, we were able to actually view the paths of the rays of light in detail and notice better results.

3 Modelling Results

3.1 Implementation

3.1.1 Software Used

Our group is using **MATLAB** for the simulation. This software was chosen primarily because it features inbuilt ODE solvers such as `ode45`, which significantly simplifies the coding process. By utilizing these native solvers, we avoid the need to implement our own numerical integration methods such as Euler's method or Runge-Kutta 4, allowing us to focus more on the modelling and analysis of the system dynamics. MATLAB's easy to use plotting allowed us to create striking visuals that demonstrate the dynamics going on with light around a black hole.

ODE45

We utilised the built-in `ode45` MATLAB solver as it can straightforwardly solve second order differential equations like ours. In addition, since we have all used `ode45` in class there was minimal to learn to implement the equations, allowing us to quickly transition from modelling to visualising simulations.

`geodesic` (our `ode45` function) took a couple of parameters (`~, X, r_s, noise_scale, noise_accel`), `~ & X` were the standard time and X needed for `ode45` functions, `X` was modelled the same as X from section 2.2.2. `r_s` was the black hole radius and `noise_scale & noise_accel` were the noise parameters.

Noise was a Gaussian distribution centred on 1 and a respective standard deviation of `noise_scale & noise_accel`. `noise_accel` which were then multiplied to $\dot{r}$ and $\dot{\phi}$ in the calculations. This enabled the different runs to have different routes but not be too drastically different that the route light takes cannot be analysed. `noise_scale` was used on `f` to mimic the force from the black hole being interfered with by other masses in the vicinity, but the largest pull would be from the black hole, meaning that we did not the noise from this force to be overwhelming as that would take too much away from the black hole dynamics.

Finally, `dxdt` contained the derivatives of the four derivatives following the equations defined in section 2.2.6 and multiplying the exact values by the Gaussian noise.

3.2 Initial results

Most of the results were in the form of videos, which we believe are a better way of visualising what is happening than a still image, so in addition to the images in this report we uploaded the videos to YouTube (We recommend listening to the Interstellar soundtrack while watching these, that can be found here):

Playlist on YouTube

3.2.1 Differing starting positions

The first experiment we wanted to run was to see how a slight change in starting position can affect the path that the light takes around a black hole. These can be seen in figure 4, in Figure 4a the light arrives in the general vicinity of the black hole and bends around it but never getting too close that it gets drawn into the black hole, even moving slightly closer like in

Figure 4b causes the light to leave the orbit of the black hole in the complete opposite direction than it arrived. But moving only another half down in Figure 4c and now the light dances on the boundary of the photon sphere, completing a whole circuit and then leaving the black hole into outer space. Finally, again decreasing the initial y value in 4d causes the black hole to absorb the light

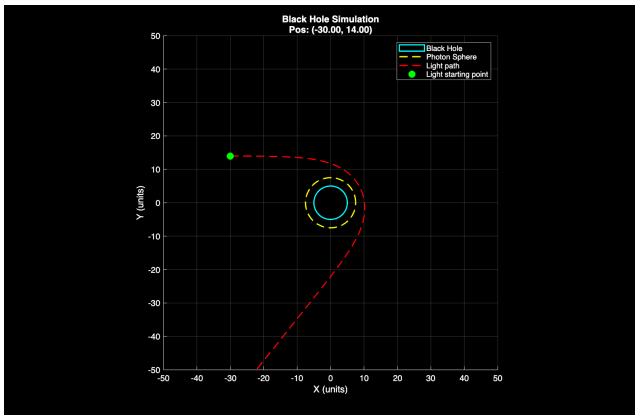

(a) Starting position of (-30, 14)

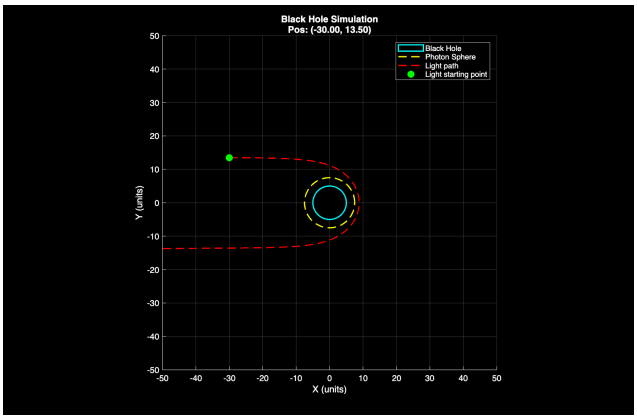

(b) Starting position of (-30, 13.5)

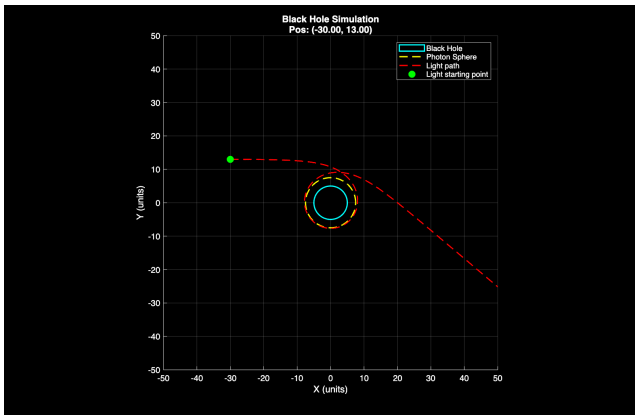

(c) Starting position of (-30, 13)

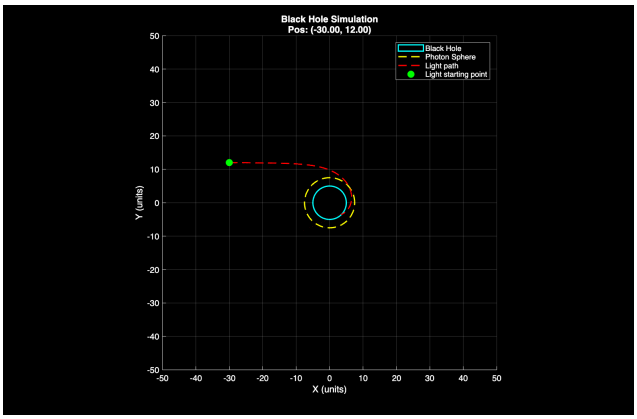

(d) Starting position of (-30, 12)

Figure 4: Figures depicting the path (red line) light takes around a black hole (yellow and blue lines) with minor differences in starting point (green point). All rays start with a 180:1 ratio in the x direction compared to the y direction.

3.2.2 Same Initial conditions

Now we know that light travelled differently around a black hole depending on its starting position, we wanted to see how the path differs from the same starting point. Due to the noise, the path will not be deterministic, mimicking real life and disturbances around the black hole.

Figure 5 draws the paths of light from a specified point (29, 20) going directly diagonally left down. These rays show the effect that the noise has on the path as sometimes it manages to completely escape and shoot off into the abyss on the other side of the black hole, but occasionally, as in Figure 5b the light perfectly goes round the photosphere at least once and then shoots off. Then, to round off the outcomes, the noise can cause the light to fall in occasionally.

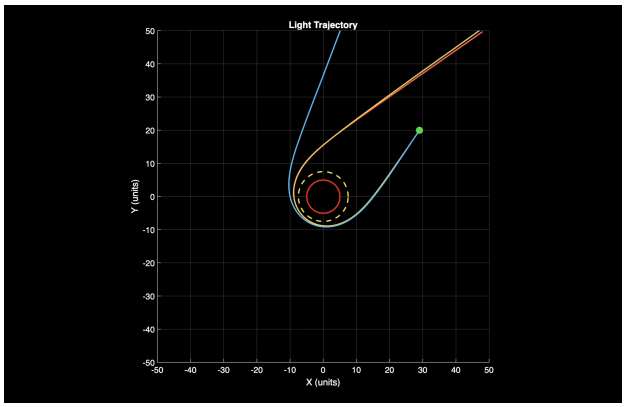

(a) Video

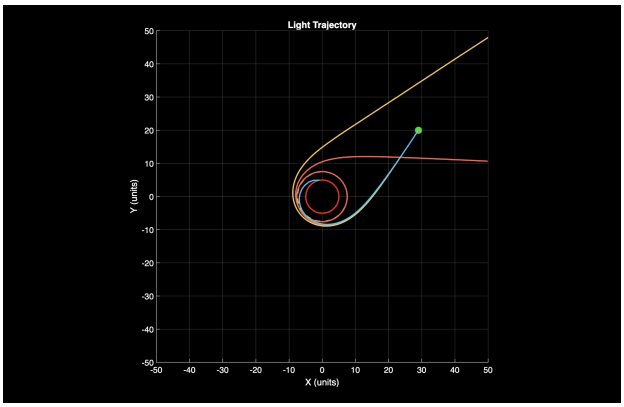

(b) Video

Figure 5: Two images demonstrating the different routes the light takes with the same initial position and direction, both figures start from the same point: (29,20) with the initial direction going directly diagonally left down.

Monte Carlo Escape test

We performed a Monte Carlo experiment, using the same points as in Figure 4, the results of which can be seen in table 1. We ran each point 1000 times and then checked if the last point was within the radius of the photon sphere. We could use the photon sphere instead of the actual black hole radius because the simulations all ran for long enough that the light would either have been drawn in or have escaped, but allows for slight numerical errors on MATLAB's end that mean the position is not under the black hole radius.

(X,Y)	Escaped	Captured	Escape Percentage
(-30, 14)	1000	0	100%
(-30, 13.5)	1000	0	100%
(-30, 13)	515	485	51.5%
(-30, 12)	0	1000	0%

Table 1: Monte Carlo escape test for the points from Figure 4.

From the first set of Monte Carlo experiments performed in 1, very interesting information comes out about the trajectories from the initial conditions. Most notably that only for (-30, 13) did the light escape and get captured, even though for (-30, 13.5) the light went very close to the photosphere. This demonstrates that even though the path can differ greatly with different initial conditions, the boundary between escaping and falling in is a very tight boundary line. To try and find out more about this boundary line we performed a second Monte Carlo experiment but with smaller ranges between the Y values, 2. We kept the X value constant at -30 and changed Y, starting at 13.5 and decreasing by 0.1 until getting to no light escaping. We can see the slight increase in falling in until the rate of escape started dropping dramatically after 13.1, indicating a rough boundary of instability for the light between 13.1 and 12.9.

3.2.3 Around a Point

The next experiment we were interested in simulating was how multiple light rays around the same point travel. Using the point (-29,20) in Figure 6 with varying densities of lines, creating a "spider" looking diagram. We will examine Figure 6b now to picture the dynamics in this

(X,Y)	Escaped	Captured	Escape Percentage
(-30, 13.5)	1000	0	100%
(-30, 13.4)	1000	0	100%
(-30, 13.3)	1000	00	100%
(-30, 13.2)	982	18	98.2%
(-30, 13.1)	865	135	86.5%
(-30, 13)	505	495	50.5%
(-30, 12.9)	130	870	13%
(-30, 12.8)	19	981	1.9%
(-30, 12.7)	3	997	0.03%
(-30, 12.6)	0	1000	0%

Table 2: Monte Carlo escape test for initial conditions, X = -30, y = [13.5, 12.6]

scenario. The pink/red lines depict the minimal effect that the black hole has on trajectories far away and going away from the black hole, as can be seen with the minimal curvature into the bottom right corner. As we start to get more round towards the black hole, the orange/yellow and dark/light blue lines, the lines start to curve more but the light is too far away to be pulled into the black hole. As we get closer to the black hole, the lines start to fold over more, with the blue and green lines intersecting. Finally, we come to the lines that trajectories take them straight to the photosphere, those not on initial directions to miss the photosphere stood no chance and got drawn in without a fight. Whereas a light blue line took a path almost around the black hole but crucially avoided falling in. From this figure, we get a good picture of how the direction you come at the black hole affects your journey around it.

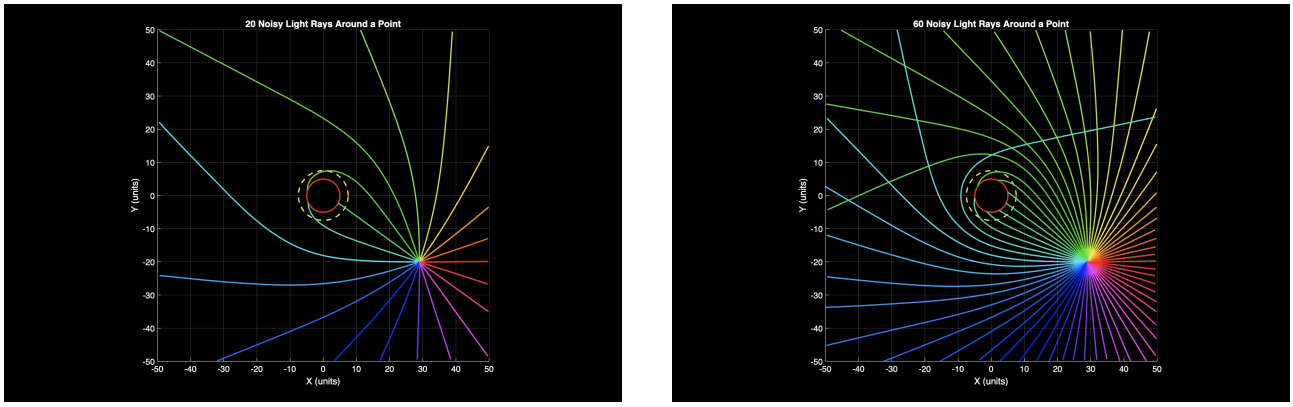

(a) 20 points, Video

(b) 60 points, Video

Figure 6: Light rays spread evenly around a circle around the point (29,-20)

3.2.4 Around a Moving Point

Now we have seen light rays around a static point, the natural next step would be to see how those paths change when the source moves, simulating a moving light source, eg a star orbiting the black hole. From figure 7 we can see that as the light source moves across the black hole, different trajectories become affected apart from the ones always aiming away from the black hole. The red lines in 7a and7b are still affected by the black hole considerably but after passing the vertical line of the black hole, the red lines become less and less affected by the black hole until there is no effect whereas the blue and green start off with minimal curvature and slowly

curve until pointing straight at the black hole in 7c. This demonstrates how from different starting positions, the trajectories can vary dramatically.

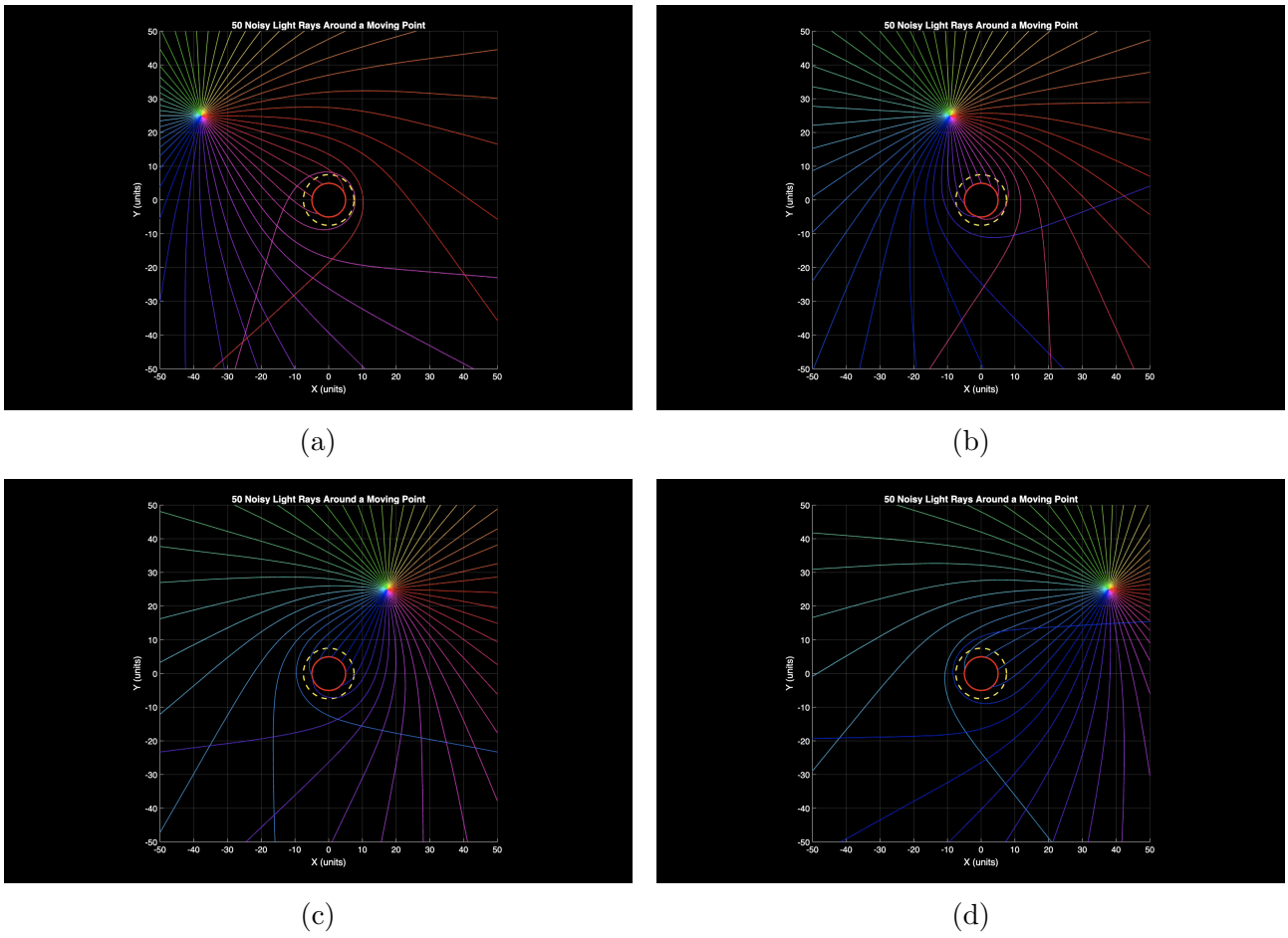

(a) (b)

(c) (d)

Figure 7: Figures depicting the paths of light around a moving source. The same colour line on different pictures corresponds to the same initial angle. The Y is fixed at 25 while the X varies by 1 each time step. ▶ Video

3.3 Simulation challenges

We faced a couple of challenges when trying to create these simulations, the first of which was that we had to have relative units of measurement as when we tried to use the real distances of light around a black hole (normally greater than 10^6 metres radius, Sagittarius A* has a Schwarzschild radius of $1.2 * 10^7$m [7]) MATLAB did not produce good results.

Another challenge was that around the edge of the photosphere, the ODEs produced such delicate numbers that to produce smooth enough lines that captured the dynamics correctly around the photosphere we had to use 1000s of time steps even though the actual time we care about was only within a small region of that at the start. This caused all simulations to take considerably longer to run, reducing the speed at which we could run simulations and get results. In addition to this numerical instability, when adding noise we had to be careful not to add too much noise because if the noise was too jagged then ODE45 took longer to solve as the equation effectively became a stiff equation which ODE45 cannot solve well.

4 Discussion and Conclusion

4.1 What Went Well

Over the course of this project, we successfully developed a simulation that models the geodesic of a light ray—representing the shortest path through the fabric of spacetime. We implemented models in both a 2D plane and a 3D spatial view. This dual approach allowed us to understand how light is warped by the gravitational field of a black hole, effectively linking theoretical physics with practical numerical results.

Additionally, the simulation successfully made use of the Schwarzschild metric to compute the Christoffel symbols. These were applied to the geodesic equation to form a system of coupled second-order ODE's, which were solved using MATLAB's `ode45` solver. A key achievement was the implementation of random noise. By adding Gaussian noise into the system, we were able to model gravitational perturbations and field fluctuations. This allowed us to observe the divergence of trajectories, confirming that the model can handle non-idealized, noisy environments.

Furthermore, by gathering data from the ODE's and plotting them, the non-linear nature of the system was made apparent. We successfully demonstrated the sensitivity to initial conditions, showing how minor deviations can lead to major changes in the path itself determining whether the photon enters a stable orbit, scatters to infinity, or crosses the Schwarzschild radius.

4.2 Drawbacks

A significant limitation of this project was the inability to validate our model against real experimental data. Black holes are complex celestial bodies located at vast distances, making the observation of individual photon trajectories currently impossible. While images from telescopes do exist, they do not provide accurate trajectory data required to statistically verify a simulation of this nature. Consequently, we could not perform a direct error analysis against real-world data. Instead, validation was performed via 'code-to-code' comparison, where we benchmarked our visual outputs against simulations created from other programmers.

The simulation is based on general relativity, a field with a steep mathematical learning curve. The complexity of deriving the geodesic equations from the Schwarzschild metric required a significant allocation of project time towards theoretical understanding rather than software development. This time constraint limited the scope of the simulation; for example, we focused on understanding the equations themselves instead of going straight in to make an "interstellar" model.

For this project, we had to simplify many dimensions. We started with 2D simulations so that we could easily implement the equations and have a better understanding of how everything worked. Additionally, many key constants such as the speed of light and the gravitational constant were essentially removed from the equation. While this was done to improve numerical stability, the accuracy of the model itself did decrease. However, since we were focusing on the physical behaviours of the model rather than the numerical results itself, this was not so much an issue

4.3 Improvements for next time

Currently, we model a static black hole in the centre of our simulation. In reality, a black hole is always rotating, containing angular momentum, which causes spacetime to be warped around the body itself. This involves moving from the Schwarzchild metric to the Kerr metric which involves more complex differential equations. However, this would allow us to model asymmetric orbits and the Penrose process which allows the extraction of energy from rotating black holes

Additionally, we could also implement higher-order numerical integration techniques to improve the accuracy of our photon trajectories over long distances. MATLAB works well for short paths; however, over time the error accumulates, which break the rules of energy conservation. By implementing higher order integrators, we can model orbital mechanics to accurately conserve energy throughout the simulation, preventing the light rays from artificially drifting off course.

Furthermore, we would want to model and simulate in three dimensions if we got another chance. This would help us understand the appearance of the black hole better, as a 3D model would allow us to demonstrate regions of the black hole such as the accretion disk with a closer similarity to the real world.

A final improvement that could be made is moving from representing individual photon paths to ray tracing models. This would involve setting up a virtual camera to simulate a full image enabling us to view parts such as the accretion disk and shadow of the black hole.

5 Appendix: Program Code

All our code is available on this repository:

 **https://github.com/ItzSmudge/modsim-coursework**

6 References

References

[1] C. Nolan, *Interstellar*, Paramount Pictures, 2014.
https://www.imdb.com/title/tt0816692/

[2] O. James, E. von Tunzelmann, P. Franklin, and K. S. Thorne, "Gravitational Lensing by Spinning Black Holes in Astrophysics, and in the Movie Interstellar," *Classical and Quantum Gravity*, 2015.
https://doi.org/10.48550/arXiv.1502.03808

[3] K. S. Thorne, "The Science of Interstellar," 2014.
Escalante,Kevin.KipThorne,ChristopherNolan-TheScienceofInterstellar.

[4] Event Horizon Telescope Collaboration, "First M87 Event Horizon Telescope Results. I. The Shadow of the Supermassive Black Hole," *The Astrophysical Journal Letters*, 2019.
https://iopscience.iop.org/article/10.3847/2041-8213/ab0ec7

[5] Event Horizon Telescope Collaboration, "First Sagittarius A* Event Horizon Telescope Results," 2022.
https://doi.org/10.48550/arXiv.2311.09484

[6] Simulating Black Holes in C++ - Kavan
https://www.youtube.com/watch?v=8-B6ryuBkCM

[7] O. Lutz, "Telescopes Get Extraordinary View of Milky Way's Black Hole," NASA JPL Education, 2022.
https://www.jpl.nasa.gov/edu/resources/teachable-moment/
telescopes-get-extraordinary-view-of-milky-ways-black-hole/